We are IntechOpen, the world's leading publisher of Open Access books Built by scientists, for scientists

4,800
Open access books available

122,000
International authors and editors

135M
Downloads

Our authors are among the

154
Countries delivered to

TOP 1%
most cited scientists

12.2%
Contributors from top 500 universities

CLARIVATE ANALYTICS BOOK CITATION INDEX INDEXED

WEB OF SCIENCE™

Selection of our books indexed in the Book Citation Index in Web of Science™ Core Collection (BKCI)

Interested in publishing with us?
Contact book.department@intechopen.com

Numbers displayed above are based on latest data collected.
For more information visit www.intechopen.com

13

On transpose Jacobian control for monocular fixed-camera 3D Direct Visual Servoing

Rafael Kelly[1], Ilse Cervantes[2], Jose Alvarez-Ramirez[3], Eusebio Bugarin[1] and Carmen Monroy[4]

[1]*Centro de Investigación Científica y de Educacion Superior de Ensenada,*
[2]*Instituto Potosino de Investigación Científica y Tecnológica,*
[3]*Universidad Autónoma Metropolitana,* [4]*Instituto Tecnológico de la Laguna*
Mexico

1. Introduction

This chapter deals with direct visual servoing of robot manipulators under monocular fixed-camera configuration. Considering the image-based approach, the complete nonlinear system dynamics is utilized into the control system design. Multiple coplanar object feature points attached to the end-effector are assumed to introduce a family of transpose Jacobian based control schemes. Conditions are provided in order to guarantee asymptotic stability and achievement of the control objective. This chapter extends previous results in two direction: first, instead of only planar robots, it treats robots evolving in the 3D Cartesian space, and second, a broad class of controllers arises depending on the free choice of proper artificial potential energy functions. Experiments on a nonlinear direct-drive spherical wrist are presented to illustrate the effectiveness of the proposed method.

Robots can be made flexible and adaptable by incorporating sensory information from multiple sources in the feedback loop (Hutchinson et al., 1996), (Corke, 1996). In particular, the use of vision provides of non-contact measures that are shown to be very useful, if not necessary, when operating under uncertain environments. In this context, visual servoing can be classified in two configurations: Fixed-camera and camera-in-hand. This chapter addresses the fixed-camera configuration to visual servoing of robot manipulators.

There exists in the literature a variety of visual control strategies that study the robot positioning problem. Some of these strategies deal with the control with a single camera of planar robots or robots constrained to move on a given plane (Espiau, 1992), (Kelly, 1996), (Maruyama & Fujita, 1998), (Shell et al., 2002), (Reyes & Chiang, 2003). Although a number of practical applications can be addressed under these conditions, there are also applications demanding motions in the 3D Cartesian space. The main limitation to

Work partially supported by CONACYT grant 45826

extend these control strategies to the non-planar case is the extraction of the 3D pose of the robot end-effector or target from a planar image. To overcome this problem several monocular and binocular strategies have been reported mainly for the camera-in-hand configuration, (Lamiroy et al., 2000), (Hashimoto & Noritsugu, 1998), (Fang & Lin, 2001), (Nakavo et al., 2002). When measuring or estimating 3D positioning from visual information

there are several performance criteria that must be considered. An important performance criterion that must be considered is the number and configuration of the image features. In particular, in (Hashimoto & Noritsugu, 1998), (Yuan, 1989) a minimum point condition to guarantee a nonsingular image Jacobian is given.

Among the existing approaches to solve the 3D regulation problem, it has been recognized that image-based schemes posses some degree of robustness against camera miscalibrations. It is worth noticing, that most reported 3D control strategies satisfy one of the following characteristics: 1) the control law is of the so-called type "kinematic control", in which the control input are the joint velocity instead the joint torques), (Lamiroy et al., 2000, (Fang & S-K. Lin, 2001), (Nakavo et al., 2002); 2) the control law requires the computation of the inverse kinematics of the robot (Sim et al., 2002). These approaches have the disadvantage of neglecting the dynamics of the manipulator for control design purposes or may have the drawback of the lack of an inverse Jacobian matrix of the robot.

In this chapter we focus on the fixed-camera, monocular configuration for visual servoing of robot manipulators. Specifically, we address the regulation problem using direct vision feedback into the control loop. Following the classification in (Hager, 1997), the proposed control strategy belongs to the class of controllers having the following features: **a)** direct visual servo where the visual feedback is converted to joint torques instead of joint or Cartesian velocities; **b)** endpoint closed-loop system where vision provides the end-effector and target positions, and **c)** image-based control where the definition of the servo errors is taken directly from the camera image.

Specifically, a family of transpose Jacobian control laws is introduced which is able to provide asymptotic stability of the controlled robot and the accomplishment of the regulation objective. In this way, a contribution of this note is to extend the results in (Kelly, 1996) to the non-planar case and to establish the conditions for such an extension. The performances of two controllers arose from the proposed strategy are illustrated via experimental work on a 3 DOF direct-drive robot wrist.

The chapter is organized in the following way. Section II provides a brief description of the robot manipulator dynamics and kinematics. Section III describes the camera-vision system and presents the control problem formulation. Section IV introduces a family of control systems based in the transpose Jacobian control philosophy. Section V is devoted to illustrate the performance of the proposed controllers via experimental work. Finally, Section VI presents brief concluding remarks.

Notations. Throughout this chapter, $\|\cdot\|$ denotes the Euclidean norm, x^T denotes the transpose of vector x, and $\nabla_x s(x)$ denotes the gradient of the scalar differentiable function $s(x)$.

2. Robot dynamics and kinematics

The dynamics of a n-DOF robot manipulator moving in the 3D Cartesian space is given by (Sciavicco & Siciliano, 1996)

$$M(q)\ddot{q} + C(q,\dot{q})\dot{q} + g(q) = \tau \tag{1}$$

where $q \in \Re^n$ is the vector of joint positions, $\tau \in \Re^n$ is the vector of applied joint torques, $M(q) \in \Re^{n\times n}$ is the symmetric and positive definite inertia matrix, $C(q,\dot{q}) \in \Re^{n\times n}$ is the matrix

associated to the Coriolis/centrifugal torques, and $g(q) \in \Re^n$ is the vector of gravitational torques originated by the gravitational potential function $\mathsf{U}_g(q)$ ($i.e.$ $g(q) = \nabla_q \mathsf{U}_g(q)$). The configuration space where the admissible joint coordinates lie is denoted by $\mathsf{C} \subset \Re^n$.

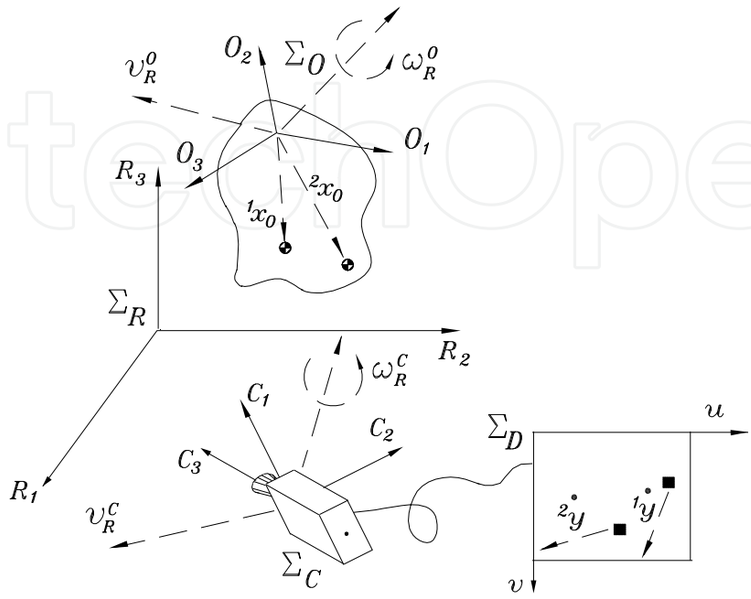

Figure 1. General differential imaging model

On the other hand, consider a fixed *robot* frame Σ_R and a moving frame Σ_O attached at the robot end-effector grasping an object which is assumed to be a rigid body (see Figure 1). The position of the end-effector (object) frame Σ_O relative to Σ_R is denoted by $O_R^O(q)$ and the corresponding rotation matrix by $R_R^O(q)$. A local description for the pose (position and orientation) of the end-effector frame is considered by using a minimal representation of the orientation. In this way, it is possible to describe the end-effector frame Σ_O pose by means of a vector $s \in \Re^m$ with $m \leq 6$:

$$s = s(q)$$

where $s(q)$ represents the direct kinematics. We regard to the robot, this chapter assumes that it is nonredundant in the sense $m = n$.

The *differential kinematics* describes the Cartesian end-effector velocity as a function of the joint velocity $\dot{q}$. Let ϑ_R^O and ω_R^O be the linear and angular velocity, respectively, of the frame Σ_O with respect to Σ_R. They are related to the joint velocity via the robot differential kinematics

$$\begin{bmatrix} \vartheta_R^O \\ \omega_R^O \end{bmatrix} = J_G(q)\dot{q}$$

where $J_G(q) \in \mathrm{I}R^{6\times n}$ is the robot geometric Jacobian.

The nonsingular robot configurations are the subset of the configuration space C where the robot Jacobian is full rank, that is

$$\mathsf{C}_{NS} = \{q \in \mathsf{C} : \mathrm{r}ank\{J_G(q)\} = n\}.$$

It is convenient to define the set of admissible nonsingular end-effector poses as

$$\mathsf{P} = \{s \in \Re^n : \exists\, q \in \mathsf{C}_{NS} : s = s(q)\}.$$

At regular configurations $q \in \mathsf{C}_{NS}$ of nonredundant robots, there exists no self-motion around these configurations. Thus, no regular configurations can lie on a continuous path in the configuration space that keeps the kinematics function at the same value (Seng et al., 1997). This yields the following

Lemma 1. For nonredundant robots and an admissible end-effector pose $p \in \mathsf{P}$, the corresponding solutions $q \in \mathsf{C}_{NS}$ of the inverse kinematics are isolated.

3. Fixed-camera imaging model

Consider a video camera standing in a fixed place with frame Σ_C which captures images of a subspace of the robot workspace.

Moreover, Frame Σ_C is located relative to Σ_R as described by a position vector, O_R^C, and a rotation matrix, R_R^C. In order to get a confident measure of the position and orientation of the robot end-effector, the grasping object is provided with p feature points. Such points are referred as *object feature points*, denoted −with respect to Σ_O− by ${}^1x_O, {}^2x_O, \cdots, {}^px_O$. The description of the object feature points ${}^ix_O$ for $i = 1, \cdots, p$ relative to frames Σ_R and Σ_C are denoted by ${}^ix_R$ and ${}^ix_C$ respectively. For each object feature point ${}^ix_O$ there is a corresponding *image* feature point ${}^iy = [{}^iu, {}^iv]^T$.

A. Imaging model

The *imaging model* gives the image feature vector ${}^iy$ of the corresponding object features ${}^ix_O$ (referred to Σ_O). This model involves transformations and a perspective projection. The whole imaging model is described by (Hutchison, 1996)

$${}^ix_R = R_R^O(q)\,{}^ix_O + O_R^O(q) \tag{2}$$

$${}^ix_C = R_R^{CT}\left[{}^ix_R - O_R^C\right] \tag{3}$$

$${}^iy = \frac{\lambda\,\alpha}{{}^ix_{C_3} - \lambda}\begin{bmatrix} {}^ix_{C_1} \\ {}^ix_{C_2} \end{bmatrix} - \alpha\begin{bmatrix} O_{I_1} \\ O_{I_2} \end{bmatrix} + \begin{bmatrix} u_0 \\ v_0 \end{bmatrix} \tag{4}$$

where α is a scale factor, λ is the lens focal length, $[O_{I_1} \;\; O_{I_2}]^T$ is the image plane offset and $[u_0 \;\; v_0]^T$ is the image center.

It is worth noticing that the model requires the robot kinematics $s(q)$ in terms of $R_R^O(q)$ and $O_R^O(q)$. Hence, the image feature point ${}^iy$ is a function of the end-effector pose s and finally

of the joint position vector q. With abuse of notation, when required ${}^{i}y(s)$ or ${}^{i}y(q)$ may be written.

According to the exterior orientation calibration problem addressed in (Yuan, 1989), in general the computation of the pose of a rigid object in the 3D Cartesian space relative to a camera based in the 2D image of known coplanar feature points located on the object is solved by using 4 noncollinear feature points. A consequence of this result is stated in the following

Lemma 2. Consider the *extended* imaging model corresponding to p points

$$\begin{bmatrix} {}^{1}y \\ \vdots \\ {}^{p}y \end{bmatrix} = \begin{bmatrix} {}^{1}y(s) \\ \vdots \\ {}^{p}y(s) \end{bmatrix}.$$

At least $p=4$ coplanar but noncollinear points are required generically to have isolated end-effector pose s solutions of the inverse extended imaging model.

Due to this result, the following assumption is in order A1 Attached to the object are $p=4$ coplanar but noncollinear feature points.

B. Differential imaging model

The *differential imaging model* describes how the image feature ${}^{i}y$ changes as a function of the joint velocity q. This is obtained by differentiating the imaging model which after tedious by straightforward manipulations can be written as

$$ {}^{i}\dot{y} = A_i({}^{i}y, {}^{i}x_{C_3}, q, {}^{i}x_O)q \tag{5}$$

where matrix $A_i(\cdot) \in \Re^{2\times n}$ is given in (6) at the top of next page. $J_{image}(\cdot) \in \Re^{2\times 6}$ in (7) denotes the image Jacobian (Hutchinson et al., 1996) where the focal length λ was neglected (i.e. ${}^{i}x_{C_3} - \lambda = {}^{i}x_{C_3}$) and the misalignment vector O_I was absorbed by the computer image center vector $[u_0 \;\; v_0]^T$. The matrix $S(\cdot) \in \Re^{3\times 3}$ is a skew-symmetric matrix defined as

$$S(x) = \begin{bmatrix} 0 & -x_3 & x_2 \\ x_3 & 0 & -x_1 \\ -x_2 & x_1 & 0 \end{bmatrix}.$$

C. Control objective

For the sake of notation, define the *extended* image feature vector $y \in \Re^8$ and the *desired* image feature vector $y_d \in \Re^8$ as

$$y = \begin{bmatrix} {}^{1}y \\ {}^{2}y \\ {}^{3}y \\ {}^{4}y \end{bmatrix} \quad \text{and} \quad y_d = \begin{bmatrix} {}^{1}y \\ {}^{2}y_d \\ {}^{3}y_d \\ {}^{4}y_d \end{bmatrix}$$

where ${}^{i}y_d$ for $i=1,2,3,4$ are the *desired* image feature points. For convenience we define the set of admissible desired image features as

$$\mathsf{Y}_d = \left\{ y_d \in \Re^8 : \exists\, s \in \mathsf{P} : y_d = y(s) \right\}.$$

In words, the admissible desired image features are those obtained from the projection of the object feature points for any admissible nonsingular end-effector pose.
One way to get such a y_d is the "teach-by-showing" strategy (Weis et al., 1987). This approach utilizes manual positioning of the end-effector at a desired pose −neither joint position nor end-effector pose measurement is needed− and the vision system extracts the corresponding image feature points.
Let $\tilde{y} = y_d - y$ be the image feature error. The image-based control objective considered in this chapter is to achieve asymptotic matching between the actual and desired image feature points, that is

$$A_i({}^i y, {}^i x_{C_3}, q, {}^i x_O) = \left[-J_{image}({}^i y, {}^i x_{C_3})[I_3 \, 0_{3x3}] R_R^{C^T} \quad J_{image}({}^i y, {}^i x_{C_3})[I_3 \, 0_{3x3}] R_R^{C^T} S(R_R^O(q)\, {}^i x_O) \right] J_G(q) \tag{6}$$

$$J_{image}({}^i y, {}^i x_{C_3}) = \begin{bmatrix} -\dfrac{\alpha\lambda}{{}^i x_{C_3}} & 0 & \dfrac{{}^i u - u_0}{{}^i x_{C_3}} & \dfrac{[{}^i u - u_0][{}^i v - v_0]}{\alpha\lambda} & -\alpha\lambda - \dfrac{[{}^i u - u_0]^2}{\alpha\lambda} & [{}^i v - v_0] \\ 0 & -\dfrac{\alpha\lambda}{{}^i x_{C_3}} & \dfrac{{}^i v - v_0}{{}^i x_{C_3}} & \alpha\lambda + \dfrac{[{}^i v - v_0]^2}{\alpha\lambda} & -\dfrac{[{}^i u - u_0][{}^i v - v_0]}{\alpha\lambda} & -[{}^i u - u_0] \end{bmatrix} \tag{7}$$

$$\lim_{t \to \infty} \tilde{y}(t) = 0. \tag{8}$$

It is worth noticing that in virtue of assumption A1 about the selection of 4 coplanar but noncollinear object feature points and Lemma 2, the end-effector poses s that yield $\tilde{y} = 0$ are isolated and they are nonsingular. On the other hand, this conclusion and Lemma 1 allow to affirm that the corresponding joint configurations q achieving such poses is also isolated and nonsingular. This is summarized in the following
Lemma 3 The joint configuration solutions $q \in \mathsf{C}_{NS}$ of

$$\tilde{y}(s(q)) = 0 \tag{9}$$

are isolated.
For convenience, define the nonempty set Q as the collection of such points −isolated solutions−, that is,

$$\mathsf{Q} = \left\{ q \in \mathsf{C}_{NS} : \tilde{y}(s(q)) = 0 \right\}.$$

Therefore, the following equivalence arises straightforwardly

$$\tilde{y}(s(q)) = 0 \Leftrightarrow q \in \mathsf{Q}. \tag{10}$$

4. Transpose Jacobian Control

In order to solve the control problem stated above, we have focus our selves on the so-called Transpose Jacobian (TJ) control schemes originally introduced by (Takegaki & Arimoto, 1981). Such controllers have the advantage of non-requiring the robot's inverse kinematics

nor the inverse Jacobian matrix. Motivated by (Kelly, 1996), the objective of this section is to propose a family of TJ controllers which be able to attain the control objective (8).
For the sake of notation, define the *extended* Jacobian $J(q)$ as

$$J(q) = \begin{bmatrix} A_1(q) \\ A_2(q) \\ A_3(q) \\ A_4(q) \end{bmatrix} \in \Re^{8\times n}$$

where with abuse of notation $A_i(q) = A_i({}^i y, {}^i x_{C_3}, q, {}^i x_O)$.
On the other hand, notice that the *extended* differential imaging model can be written as

$$y = J(q)q. \tag{11}$$

Inspired from (Kelly, 1996), (Takegaki & Arimoto, 1981), (Miyazaki & Arimoto, 1985), (Kelly, 1999), we propose the following class of transpose Jacobian-based control laws

$$\tau = J(q)^T \nabla_y \mathsf{U}(y) - K_v \dot{q} + g(q), \tag{12}$$

where $\mathsf{U}(y)$ is a continuously differentiable positive definite function called *artificial potential energy*, and $K_v \in \Re^{n\times n}$ is a symmetric positive definite matrix.
We digress momentarily to establish the following result whose proof is in the appendix.
Lemma 4. Consider the equation

$$J(q)^T \nabla_y \mathsf{U}(y(q)) = 0.$$

Then, each $q^* \in \mathsf{Q}$ is an isolated solution, that is there exists $\delta > 0$ such that in $\|q^* - q\| < \delta$

$$J(q)^T \nabla_y \mathsf{U}(y(q)) = 0 \Leftrightarrow q = q^*.$$

The main result of this chapter is stated in the following
Proposition 1. Consider the robot camera-system (1)-(5) and the family of transpose Jacobian control schemes (12). Then, the closed-loop control system satisfies the control objective (8) locally.
Proof: The closed-loop system analysis is carried out by invoking the Krasovskii−LaSalle's theorem. The theorem statement is presented in (Vidyasagar, 1993) ; this allows to study asymptotic stability of autonomous systems.
The closed-loop system dynamics is obtained by substituting the control law (12) into the robot dynamics (1). This leads to the autonomous system

$$M(q)\ddot{q} + C(q,\dot{q})\dot{q} = J(q)^T \nabla_y \mathsf{U}(y) - K_v \dot{q} \tag{13}$$

which can be written as

$$\frac{d}{dt}\begin{bmatrix} q \\ \dot{q} \end{bmatrix} = \begin{bmatrix} \dot{q} \\ M(q)^{-1}\left[J(q)^T \nabla_y \mathsf{U}(y(q)) - K_v \dot{q} - C(q,\dot{q})\dot{q}\right] \end{bmatrix}.$$

Since the artificial potential energy $\mathsf{U}(\tilde{y})$ was assumed to be positive definite, then it has an isolated minimum point at $\tilde{y}=0$, so its gradient $\nabla_{\tilde{y}}\mathsf{U}(\tilde{y})$ has an isolated critical point at $\tilde{y}=0$. This implies that it vanishes at the isolated point $\tilde{y}=0$.

Therefore, in virtue of (10) we have that $[q^T \;\; \dot{q}^T]^T = \begin{bmatrix} q^T & 0^T \end{bmatrix}^T$ with $q \in \mathsf{Q}$ are equilibria of the closed-loop system. Furthermore, because the elements of Q are isolated, then the corresponding equilibria are isolated too. However, other equilibria may be possible for $q \notin \mathsf{Q}$ whether $J(q)^T \nabla_{\tilde{y}} \mathsf{U}(\tilde{y}(q)) = 0$.

Let q^* be any point in Q and define a region D around the isolated equilibrium $[q^T \;\; \dot{q}^T]^T = [q^{*T} \;\; 0^T]^T$ as

$$D = \left\{ \begin{bmatrix} q \\ \dot{q} \end{bmatrix} \in \mathsf{C} \times \Re^n : \left\| \begin{matrix} q^* - q \\ \dot{q} \end{matrix} \right\| < \varepsilon \right\}$$

where $\varepsilon > 0$ is sufficiently small constant such that a unique equilibrium lie in D, and in the region D the artifical potential energy $\mathsf{U}(\tilde{y}(q))$ be positive definite with respect to $q^* - q$.

As a consequence, in the set $\left\{ q : \left\| q^* - q \right\| < \varepsilon \right\}$, the unique solution of $J(q)^T \nabla_{\tilde{y}} \mathsf{U}(\tilde{y}(q)) = 0$ is $q = q^*$.

To carry out the stability analysis of the equilibria $[q^T \;\; \dot{q}^T]^T = [q^{*T} \;\; 0^T]^T$, consider the following Lyapunov function candidate

$$V(q^* - q, \dot{q}) = \frac{1}{2} \dot{q}^T M(q) \dot{q} + \mathsf{U}(\tilde{y}(q))$$

which is a positive definite function in D.

The time-derivative of $V(q, \dot{q})$ along the trajectories of the system (13), is

$$\dot{V}(q, \dot{q}) = -\dot{q}^T K_v \dot{q}$$

where $\dot{\tilde{y}} = -J\dot{q}$ and the property $\dot{q}^T \left[\frac{1}{2} \dot{M}(q) - C(q, \dot{q}) \right] \dot{q} = 0$ have been used.

Since by design matrix K_v is negative definite, hence $\dot{V}(q, \dot{q})$ is negative semidefinite function in D. In agreement with the Lyapunov's direct method, this is sufficient to guarantee that the equilibria $[q^T \;\; \dot{q}^T]^T = [q^{*T} \;\; 0^T]^T$ with $q^* \in \mathsf{Q}$ are stable.

Furthermore, the autonomous nature of the closed-loop system (13) allows the use of the Krasovskii−LaSalle's theorem (Vidyasagar, 1993) to study asymptotic stability. Accordingly, define the set

$$\begin{aligned} \Omega &= \left\{ \begin{bmatrix} q \\ \dot{q} \end{bmatrix} \in D : \dot{V}(q, \dot{q}) = 0 \right\}, \\ &= \left\{ q \in \mathsf{C} : \left\| q^* - q \right\| < \varepsilon ; \dot{q} = 0 \right\} \end{aligned}$$

The next step is to find the largest invariant set in Ω. Since in Ω we have $\dot{q} = 0$, therefore from the closed-loop system (13) it remains to determine the constant solutions q satisfying

$\|q^* - q\| < \varepsilon$ and $J(q)^T \nabla_{\tilde{y}} \mathsf{U}(\tilde{y}(q)) = 0$. As already shown in Lemma 4, if the region D is enough small, then the unique solution is $q = q^*$.

Since ε was selected such that no equilibria exists in D other than

Following arguments in (Kelly, 1999), we utilize the fact that $\mathsf{U}(\tilde{y})$ is a nonnegative function with respect to $\tilde{y}$. As a consequence of (9) we have the important conclusion that $\mathsf{U}(\tilde{y}(q))$ has minimum points if and only if $q \in \mathsf{Q}$.

This proves that the equilibria $[q^T \ \dot{q}^T]^T = [q^{*T} \ \ 0^T]^T$ with $q^* \in \mathsf{Q}$ are locally asymptotically stable, so they are attractive. As a consequence, $\lim_{t\to\infty} q(t) = q^*$, thus invoking (10) the control objective (8) is achieved. This concludes the proof.

Remark 1. So far, one objective of this chapter has been to make an extension of the existing results on transpose Jacobian controllers to the case of a 3D position and orientation. It is well known that a drawback of such control strategies is that they induce a steady-state error under uncertain gravitational torques. We propose the following control law

$$\tau = J^T \left[K_P \tilde{y} + K_I \int_0^t \tilde{y}(\sigma)\, d\sigma \right] - K_v q + \hat{\mathrm{g}}(q) \tag{14}$$

where K_I is a diagonal positive definite matrix of suitable dimensions and $\hat{g}(q)$ is the available estimate of the gravitational torques. It can be shown that the use of low integral gains in control law (14) guarantees the asymptotic stability of closed-loop system and the accomplishment of the control objective (8) in spite of uncertain gravitational torques. Furthermore, notice that if in the control law (14), $\hat{g}(q) = 0$ is chosen, the controller becomes a class of PID controller with a PI visual action and joint-coordinate damping. It can be shown also that the region of attraction of the controller (12) increases as the integral gain $K_I = \varepsilon \overline{K}_I$ decreases, being the main limitation to enlarge this region, the singularities of the Jacobian matrix J.

Remark 2. In practice, the Jacobian matrix J can be uncertain due to uncertain manipulator kinematics, camera position and orientation, and camera intrinsic parameters. In such a case, only an estimate $\hat{J}$ is available. It can be shown that by following the analysis methodology due to (Deng et al., 2002), (Cheah et al., 2003), (Cheah & Zhao, 2004) one can conclude that the feedback control law (12) (alternately (14)) can tolerate small deviation of the Jacobian matrix in the sense that

$$\|J - \hat{J}\| \le \rho$$

with ρ sufficiently small and $\|\cdot\|$ the induced matrix norm, in a neighborhood of the operating point. In the following section, we will show experimental runs to illustrate the performance of the controller for this case.

Remark 3. In the case of redundant robots $n > 6$, it may not exist a unique equilibrium point in joint space even if the control objective (8) is attained. In such case a space of dimension $n-6$ may be arbitrarily assigned. In that case, asymptotic stability to a invariant set (instead to a point) can only be concluded. This means that phenomena such as self-motion may be present.

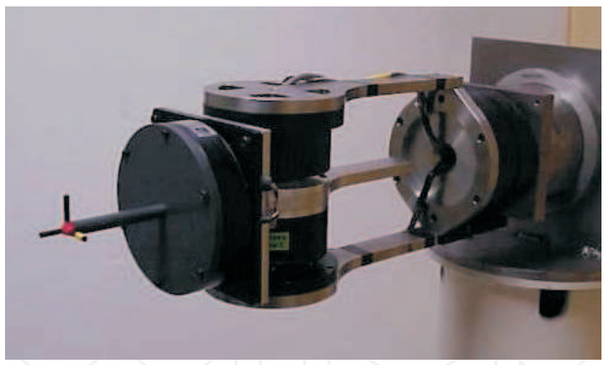

Figure 2. Direct--drive spherical wrist

5. Experiments

This section is devoted to show the experimental evaluation of the proposed control scheme. The experimental setup is composed by a vision system and a direct-drive nonlinear mechanism.

Image acquisition and processing was performed using a Pentium based computer working at 450 MHz under Linux. The image acquisition was performed using a Panasonic GP-MF502 camera model coupled to a TV acquisition board. Image processing consisted of image thresholding and detection of an object position through the determination of its centroid. As shown in Figure 3, the four object feature points are on a plane attached at the end-effector. Their position with respect to the end-effector frame is

$$
\begin{aligned}
{}^{1}x_O &= [-0.031 \;\; 0.032 \;\; 0]^T [\mathrm{m}], \\
{}^{2}x_O &= [0.036 \;\; 0.037 \;\; 0]^T [\mathrm{m}], \\
{}^{3}x_O &= [-0.034 \;\; -0.033 \;\; 0]^T [\mathrm{m}], \\
{}^{4}x_O &= [0.032 \;\; -0.035 \;\; 0]^T [\mathrm{m}].
\end{aligned}
$$

Figure 3 also shows four marks `+' corresponding to the desired image features obtained following the "teach-by-showing" strategy; they are given by

$$
\begin{aligned}
{}^{1}y_d &= [364 \;\; 197]^T [\mathrm{p}ixels], \\
{}^{2}y_d &= [353 \;\; 157]^T [\mathrm{p}ixels], \\
{}^{3}y_d &= [403 \;\; 208]^T [\mathrm{p}ixels], \\
{}^{4}y_d &= [394 \;\; 171]^T [\mathrm{p}ixels].
\end{aligned}
$$

The capture of the image and the extracted information are updated at the standard rate of 30 frames per second. The centroid data is transmitted to the mechanism control computer via the standard serial port.

The camera intrinsic parameters are the following: $\lambda = 0.008$ [m], $\alpha = 72000$ [pixels/m], $u_0 = 320$ [pixels], $v_0 = 240$ [pixels] y $O_I = 0$. The camera pose during the experimental tests was

$$
O_R^C = [0 \;\; 0 \;\; 1.32]^T [\mathrm{m}],
$$

for its position and the following rotation matrix for the orientation

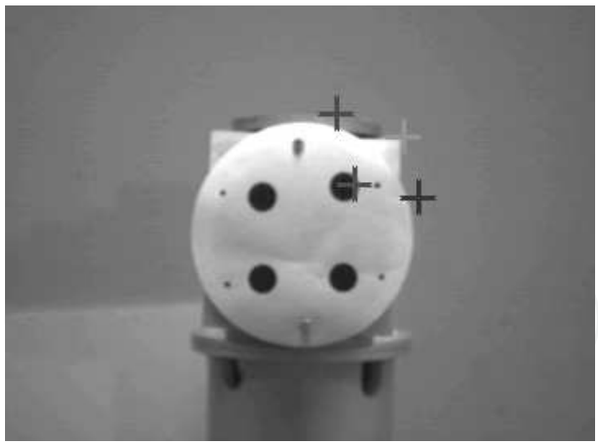

Figure 3. Initial configuration `●′ and desired image feature points `+′

$$R_R^C = [1000 - 1000 - 1].$$

The robot manipulators is a direct-drive 3 degrees of freedom spherical wrist shown in Figure 2. This direct-drive wrist was built at CICESE Research Center and it is equipped with joint position sensors, motor drivers, a host computer and software environment which generates a user-friendly interface. Further information regarding the robot wrist can be found in **Error! Reference source not found.**. The geometric Jacobian is given by

$$J_G = \begin{bmatrix} -ds_1 s_2 & dc_1 c_2 & 0 \\ dc_1 s_2 & ds_1 c_2 & 0 \\ 0 & -ds_2 & 0 \\ 0 & -s_1 & c_1 s_2 \\ 0 & c_1 & s_1 s_2 \\ 1 & 0 & c_2 \end{bmatrix}$$

which has singular configurations at $q_2 = n\pi$.

A. PD transpose Jacobian control

Consider the following global positive definite artificial potential energy function

$$\mathsf{U}(\tilde{y}) = \frac{1}{2}\tilde{y}^T K_p \tilde{y}$$

where $K_p \in \Re^8 \times 8$ is a symmetric positive definite matrix. Since its gradient is $\nabla_{\tilde{y}} \mathsf{U}(\tilde{y}) = K_p \tilde{y}$, so the control law (12) becomes the PD transpose Jacobian control

$$\tau = J(q)^T K_p \tilde{q} - K_v \dot{q} + g(q) \tag{15}$$

where $K_v \in \Re^{n \times n}$ is a symmetric positive definite matrix.

The controller parameters were chosen by a tedious trail and error procedure in such a way to obtain the smaller steady state imaging error by keeping two practical constraints: maintaining the control actions within the actuator torque capabilities and avoiding large velocities to allow the vision system compute the centroids at the specified rate. The experiments were conducted with $K_p = \mathrm{d}iag\{5,5,5,1,1,3,5,5\} \times 10^{-4}$ and $K_v = \mathrm{d}iag\{0.9,0.7,0.17\}$.

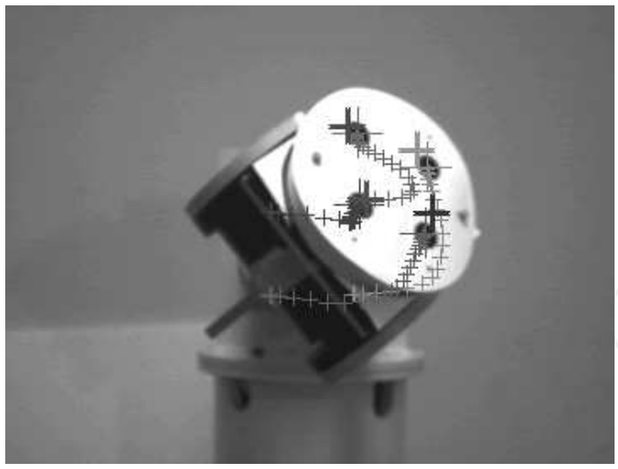

Figure 4. Trace of the image feature points: PD transpose Jacobian control

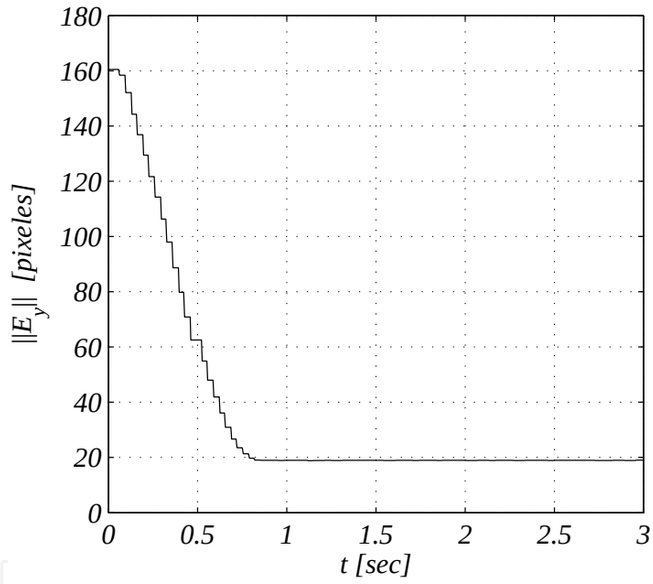

Figure 5. Norm of the image feature error: PD transpose Jacobian control

B. Tanh-D transpose Jacobian control

To deal with friction at the robot joint, let us consider the following artificial potential energy function (Kelly, 1999), (Kelly et al., 1996)

$$U(\tilde{y}) = \sum_{i=1}^{8} \frac{k_{pi}}{\lambda_i} ln\{cosh(\lambda_i \tilde{y}_i)\}$$

where k_{pi} and λ_i are positive constants. It can be shown that this is a globally positive definite function whose gradient is $\nabla_{\tilde{y}} U(\tilde{y}) = K_p tanh(\Lambda \tilde{y})$ where $K_p = diag\{k_{p1}, \cdots, k_{p8}\}$, $\Lambda = diag\{\lambda_1, \cdots, \lambda_8\} \in \Re^{8\times 8}$ are diagonal positive definite matrices. For a given vector $x \in \Re^8$, function $tanh(x)$ is defined as

$$tanh(x) = \begin{bmatrix} tanh(x_1) \\ \vdots \\ tanh(x_8) \end{bmatrix}$$

where $tanh(\cdot)$ is the hyperbolic tangent function.

With the above choice of the artificial potential energy, the control law (12) produces the Tanh-D transpose Jacobian control

$$\tau = J^T K_p tanh(\Lambda \tilde{y}) - K_v \dot{q} + g(q) \tag{16}$$

where $K_v \in \Re^{n \times n}$ is a symmetric positive definite matrix.

The first term on the right hand side of control law (16) offers more flexibility than the simpler $J^T K_p \tilde{y}$ in (15) to deal with practical aspects such as friction at the robot joints and torque limit in the robot actuators (Kelly, 1999).

The experiments were carried out with the following controller parameters $K_p = 0.015I$, $K_v = \mathrm{d}iag\{1.0, 0.7, 0.3\}$ and $\Lambda = 0.2I$.

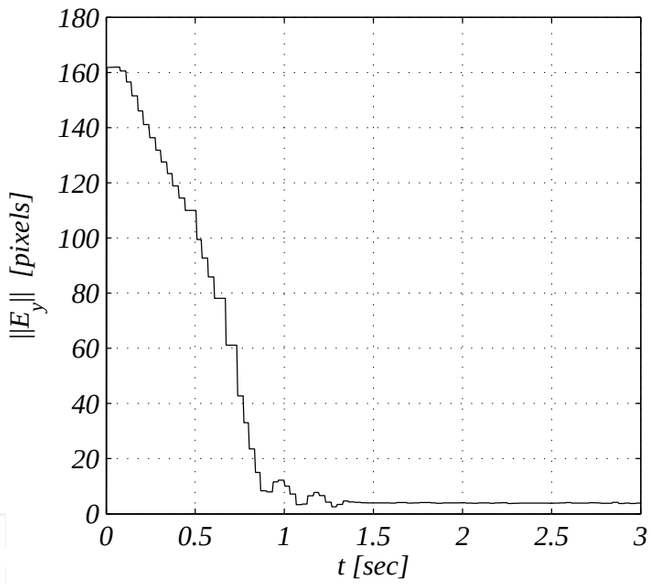

Figure 6. Norm of image feature error: Tanh-D transpose Jacobian control

Figure 6 depicts the norm of the image feature error $\tilde{y}$. Notice that the norm of the error has a smooth evolution with no overshoot reaching a steady state value of 4.0 pixels in about 1.5 seconds. Although it is expected to have asymptotically a zero error, in practice a small remaining error is present. This behavior is mainly due to uncertainties in the camera pose measurement.

C. Tanh-D approximate transpose Jacobian control

The experiment conducted with control laws (15) and (16) used complete knowledge of the experimental setup, then all the information was available to compute the extended Jacobian J. More specifically, the evolution of the deep associated at each object feature point was

computed on-line from (3) thanks to the use of the robot kinematics and measurement of joint positions q for ${}^{i}x_{R}$.

In the more realistic case where uncertainties are present in the camera calibration, then it is no anymore possible to invoke (3) for computing the deep ${}^{i}x_{C3}$ of the object feature points. This implies that the extended Jacobian J cannot be computed exactly. Notwithstanding, as pointed out previously, it is still possible to preserve asymptotic stability in case of an approximate Jacobian $\hat{J}$ be utilized in lieu of the exact one.

The experiment was carried out by utilizing a constant deep ${}^{i}x_{C3} = 0.828$ [m] for the four object feature points $i = 1,2,3,4$. This yields an approximated Jacobian $\hat{J}$ to be plugged into the control law (16)

$$\tau = \hat{J}^{T} K_{p} tanh(\Lambda \tilde{y}) - K_{v}\dot{q} + g(q).$$

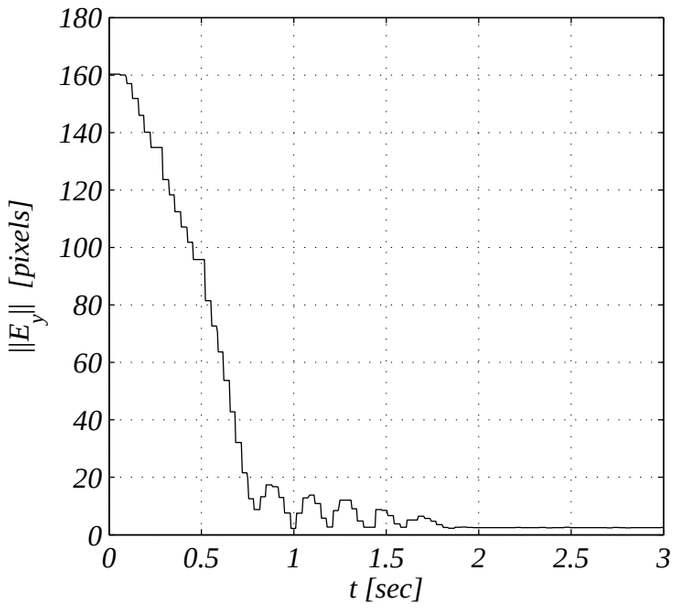

Figure 7. Norm of image feature error: Approximate Jacobian

The time evolution of the norm of the image error vector is depicted in Figure 7. It can be observed that although the response has a small oscillatory transient, it reaches an steady state error of 2.5 pixels around 2 seconds. This error is smaller than the obtained during experiments utilizing the exact Jacobian.

6. Conclusions

In this chapter we have provided some insights on the stability of robotic systems with visual information for the case of a monocular fixed-eye configuration on n DOF robot manipulators. General equations describing the fixed-camera imaging model are given and a family of transpose Jacobian control schemes is introduced to solve the regulation problem. Conditions are provided to show that such controllers guarantee asymptotic stability of the closed-loop system.

In order to illustrate the effectiveness of the proposed control schemes, experiments were conducted on a nonlinear direct-drive mechanical wrist. Both, the case of exact Jacobian as well as approximate Jacobian were evaluated. Basically they present similar performance, although the steady state image error was smaller when the approximate Jacobian was tested.

7. Appendix

Proof of Lemma 4. According to (10) we have that $q \in \mathsf{Q}$ are isolated solutions of $\tilde{y}(q) = 0$. Denote by q^* any element of Q. Since by design the artificial potential energy $\mathsf{U}(\tilde{y})$ is definite positive, then $\mathsf{U}(\tilde{y}(q))$ is definite positive with respect to $q^* - q$. This implies that $\mathsf{U}(\tilde{y}(q))$ has an isolated minimum point at $q = q^*$. Hence, its gradient with respect to q has an isolated critical point at $q = q^*$, i.e. there is $\delta > 0$ such that in $\|q^* - q\| < \delta$

$$\nabla_q \mathsf{U}(\tilde{y}(q)) = 0 \Leftrightarrow q = q^*.$$

Finally, the desired result follows from

$$\nabla_q \mathsf{U}(\tilde{y}(q)) = -J(q)^T \nabla_{\tilde{y}} \mathsf{U}(\tilde{y}(q)).$$

8. References

Hutchinson, S., Hager, G. and Corke, P. (1996), A tutorial on visual servoing. *IEEE Transactions on Robotics and Automation*, pp. 651-670, Vol. 12, No.5, 1996.

Corke, P. (1996), *Visual control of robots*, Research Studies Press Ltd.

Espiau, B., Chaumette, F. and Rives, P. (1992),A new approach to visual servoing in robotics, *IEEE Trans. on Robotics and Automation*, Vol. 8, No. 3, pp. 313-326, june 1996.

Kelly, R. (1996), Robust asymptotically stable visual servoing of planar robots. *IEEE Trans. on Robotics and Automation*, Vol. 12, pp. 759-766, October 1996 .

Maruyama, A. & Fujita, M. (1998), Robust control for planar manipulators with image feature parameter potential, *Advanced Robotics*, Vol. 12, No. 1, pp. 67-80.

Shen, Y., Xiang, G., Liu, Y. & Li, K. (2002), Uncalibrated visual servoing of planar robots, *Proc. IEEE Int. Conf. on Robotics and Automation*, Washington, DC, pp. 580-585, May 2002.

Reyes, F. & Chiang, L. (2003), Image--to--space path planning for a SCARA manipulator with single color camera, *Robotica*, Vol. 21, pp. 245-254, 2003.

***A. Behal, P. Setlur, W. Dixon and D. E. Dawson (2005), Adaptive position and orientatio regulation for the camera-in-hand problem, *Journal of Robotic Systems*, vol. 22, No. 9, pp. 457--473, September 2005.

Lamiroy, B., Puget, C. & Horaud, R. (2000), What metric stereo can do for visual servoing, *Proc. Int. Conf. Intell. Robot. Syst.*, pp. 251-256, 2000.

Hashimoto, K. & Noritsugu, T. (1998), Performance and sensitivity in visual servoing, *Proc. of the Int. Conf. on Robotics and Automation*, Leuven, Belgium, pp. 2321-2326, 1998.

Fang, C-J & Lin, S-K, (2001) A performance criterion for the depth estimation of a robot visual control system, *Proc. Int Conf. Robot. Autom*, Seoul, Korea, pp.1201-1206, 2001.

Nakavo, Y., Ishii, I. & Ishikawa, M. (2002), 3D tracking using high-speed vision systems, *Proc. Int Conf. Intell.Robot. Syst.*, Lausanne, Switzerland, pp.360-365, 2002.

Chen, J., Dawson , D. M., Dixon, W. E. & Behal, A. (2005), Adaptive Homography-Based Visual Servo Tracking for Fixed and Camera-in-Hand Configurations, *IEEE Transactions on Control Systems Technology*, Vol. 13, No. 5, pp. 814-825, 2005.

Yuan ,J., (1989) A general photogrammetric method for determining object position and orientation, *IEEE Transaction on Robotics and Automation*, Vol.5, No. 2, pp. 129-142, 1989.

Sim, T. P., Hong, G. S. & Lim, K. B. (2002), A pragmatic 3D visual servoing system *Proc. Int Conf. Robot. Autom*, Washington, D.C., USA, pp.4185-4190, 2002.

Hager, G. D. (1997) , A modular system for robust positioning using feedback from stereo vision, *IEEE Trans. on Robotics and Automation*, Vol. 13, No. 4, pp. 582-595, August 1997.

Sciavicco, L. and Siciliano, B. (1996), *Modeling and Control of Robot Manipulators*, McGraw-Hill, 1996.

Seng, J., Chen, Y. C., & O'Neil, K.A. (1997), On the existence and the manipulability recovery rate of self--motion at manipulator singularities, *International Journal of Robotics Research*, Vol. 16, No. 2, pp. 171-184, April 1997.

Weiss, L. E. , Sanderson, A. C. & Neuman, C. P. (1987), Dynamic sensor--based control of robots with visual feedback, *IEEE J. of Robotics and Automation*, Vol. 3, pp. 404-417, September 1987.

Takegaki, M., & Arimoto, S. (1981), A new feedback method for dynamic control of manipulators, *Trans. of ASME, Journal of Dynamic Systems, Measurement and Control*, vol. 102, No. 6, pp. 119-125, June 1981.

Miyazaki, F., & Arimoto, S. (1985), Sensory feedback for robot manipulators, *Journal of Robotic Systems*, Vol. 2, No. 1, pp. 53-71, 1985.

Kelly, R. (1999), Regulation of manipulators in generic task space: An energy shaping plus damping injection approach, *IEEE Trans. on Robotics and Automation*, Vol. 15, No. 2, pp. 381-386, April 1999.

Vidyasagar, M. (1993), *Nonlinear systems analysis*, Prentice Hall, 1993.

Deng, L. , Janabi-Sharifi F. & Wilson, W. (2002), Stability and robustness of visual servoing methods, *Proc. of the 2002 IEEE International Conference on Robotics and Automation*, Washington, DC, pp. 1604--1609, 11-15 May 2002.

Cheah, C.C., Hirano, M., Kawamura, S. & Arimoto, S. (2003) Approximate Jacobian Control for Robots with Uncertain Kinematics and Dynamics, *IEEE Trans. on Robotics and Automation*, Vol. 19, No. 4, pp 692- 702, 2003.

Cheah, C. & Zhao, Y. (2004), Inverse Jacobian regulator for robot manipulators: Theory and experiments, *43rd IEEE Conference on Decision and Control*, Paradise Island, Bahamas, pp. 1252-1257, December 2004.

Campa R., Kelly, R., & Santibañez, V. (2004), Windows--based real--time control of direct--drive mechanisms: Platform description and experiments, *Mechatronics*, Vol. 14, No. 9, pp. 1021-1036, November 2004 .

Kelly, R., Shirkey, P., Spong, M. W. (1996), Fixed--camera visual servo control for planar robots, *Proc. IEEE Int. Conf. on Robotics and Automation*, pp. 2643-2649, Minneapolis, Minnesota, April 1996.

Robot Manipulators

Edited by Marco Ceccarelli

ISBN 978-953-7619-06-0

Hard cover, 546 pages

Publisher InTech

Published online 01, September, 2008

Published in print edition September, 2008

In this book we have grouped contributions in 28 chapters from several authors all around the world on the several aspects and challenges of research and applications of robots with the aim to show the recent advances and problems that still need to be considered for future improvements of robot success in worldwide frames. Each chapter addresses a specific area of modeling, design, and application of robots but with an eye to give an integrated view of what make a robot a unique modern system for many different uses and future potential applications. Main attention has been focused on design issues as thought challenging for improving capabilities and further possibilities of robots for new and old applications, as seen from today technologies and research programs. Thus, great attention has been addressed to control aspects that are strongly evolving also as function of the improvements in robot modeling, sensors, servo-power systems, and informatics. But even other aspects are considered as of fundamental challenge both in design and use of robots with improved performance and capabilities, like for example kinematic design, dynamics, vision integration.

InTech Europe

University Campus STeP Ri
Slavka Krautzeka 83/A
51000 Rijeka, Croatia
Phone: +385 (51) 770 447
Fax: +385 (51) 686 166
www.intechopen.com

InTech China

Unit 405, Office Block, Hotel Equatorial Shanghai
No.65, Yan An Road (West), Shanghai, 200040, China
中国上海市延安西路65号上海国际贵都大饭店办公楼405单元
Phone: +86-21-62489820
Fax: +86-21-62489821

IntechOpen